Quantized Segmentation of Fibrotic Tissue of Left Atrial

from Delay-Enhancement MRI Images Using Level-set and Graph-cut

Xun Liu[1], Su Zhang[1]
School of Biomedical Engineering
Shanghai Jiao Tong University
Shanghai, China

Xu Zhao[2]*
Department of Automation
Shanghai Jiao Tong University
Shanghai, China
zhaoxu@sjtu.edu.cn

Yan Shen[3]
Department of Radiology
Shanghai Chest Hospital, Shanghai
Jiao Tong University
Shanghai, China

Abstract—**The pathogenesis of atrial fibrillation (AF) is closely related to the fibrotic tissues in left atrial (LA). Delay-enhancement magnetic resonance imaging (DE-MRI) has been widely used in the ablation of atrial fibrillation, which can accurately describe the distribution of myocardial fibrosis and postoperative scars. Combining EM algorithm, level-set and graph-cut, this paper proposes a method to segment the fibrotic tissues and postoperative scars and also quantify their proportion in left atrial from DE-MRI. In 4 clinical cases, our method can accomplish the extraction of heart, the segmentation of left atrium and sequentially the quantification of the fibrotic tissues nearby with little manual intervention. Experimental results show that accurate segmentation of LA is achieved in 55 slices with 96 slices containing LA among 4 cases in total. With manual correction in the rest slices, the final results about the proportion of fibrotic tissues in LA are 14.78%, 21.02%, 25.17%, 14.77% respectively which are consistent with the clinical diagnosis. Evaluated by the clinician, our method is robust against different resolution and can provide auxiliary function for ablation of AF.**

Keywords: left atrial, fibrotic tissue, Delay-enhancement MRI, segmentation, quantification.

I. INTRODUCTION

Atrial fibrillation (AF) is the most common persistent arrhythmia in clinical practice with continuously increasing prevalence and incidence[1]. AF is related to abnormal cardiac activity, contraction and structural remodeling, which result in the decrease of fiber in atrial wall and the increase of collagen composition causing the left atrial (LA) fibrosis. Catheter ablation is an effective method for the treatment of atrial fibrillation. After catheter ablation, there will be scars in LA wall, which has significant value for the evaluation and optimization of the surgical planning.

Delay-enhancement magnetic resonance imaging (DE-MRI) has been widely and successfully used for myocardial imaging, especially the ventricular myocardium imaging. A number of studies have shown that DE-MRI can accurately locate and quantify the abnormal region of ventricular myocardium [2]. By analyzing the high-resolution sequences of DE-MRI, information about fibrotic tissues and postoperative scar can be sufficiently collected, which plays an important role in guiding clinical catheter ablation. However, for clinicians, manually labeling fibrous tissue and scars in numerous slices is a time-consuming and inefficient

process with large subjectivity and low feasibility. Therefore, an automated analysis method is an urgent clinical need currently.

An important prerequisite for quantification of fibrotic tissues and postoperative scars is the segmentation of left atrial. Automated segmentation cannot be obtained easily because the shape of left atrial varies significantly in different patients and different slices of one patient, meanwhile the thin thickness of left atrial wall also results in a relative low resolution in images. Ravanelli [3] proposed a method based on threshold and registration to segment the left atrial, but this method still requires extensive manual correction by the clinician. Wachinger [4] adopted an atlas-based and contour-driven method. Tao [5] proposed an automatic segmentation method based on multiple-atlas voting from LGE-MRI and MRA. Atlas-based methods are limited when the clinical data is insufficient, and may have limited performance when the object to be segmented differs greatly with the existing knowledge.
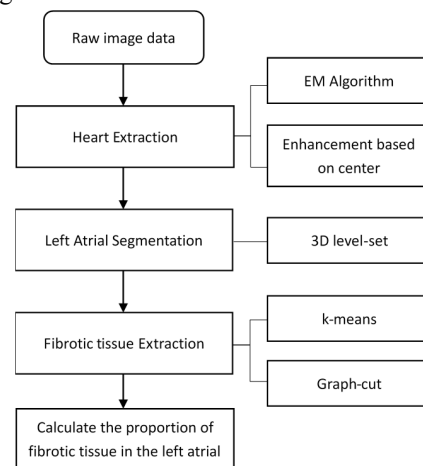

Figure 1.   Flow chart of the proposed method.

As fibrotic tissues and postoperative scars have very similar performance (high intensity) in DE-MRI, we first focus on the former. This paper aims to propose a method to quantify the fibrosis tissue with little manual intervention. From the DE-MRI images, we achieve our target by the following steps. Firstly, heart is extracted using EM algorithm combined with image enhancement. Secondly, the segmentation of LA is obtained by 3D level-set with one or

two rectangle assigned manually in one slice as initialization. This step can accomplish accurate segmentation of LA in its main body where fibrotic tissues are prone to occur. After manual correction, the whole segmentation of LA is obtained. Finally fibrosis tissues in LA wall are extracted using k-means and graph-cut, and sequentially the proportion is calculated easily. Our segmentation results of LA are proved to be prompt for clinician and the precise proportion of fibrotic tissues in LA can help choosing proper patient for the ablation surgery.

II. METHOD

As can be seen, our method is summarized in Fig.1. In the following sections, we will elaborate on each part.

A. Heart extraction based on EM algorithm and image Enhancement

According to the gray intensity, DE-MRI could be divided into three parts, the background, chest with lower intensity, the muscle and lung with medium intensity and the heart with higher intensity, as shown in Fig. 2(a). Gaussian mixture model (GMM) can reveal the characteristics of this kind of image [6]. It is a parametric probabilistic density model that assumes all the data points are generated from a mixture of finite number of Gaussian distribution components. The probability density function (PDF) of GMM is given by:

$$p(x) = \sum_{j=1}^{k} p(k)p(x|k) = \sum_{j=1}^{k} \pi_j \psi(x|u_j, \sigma_j) \quad (1)$$

where k denotes the number of single Gaussian component, namely, the number of clusters. x denotes the gray intensity of an arbitrary voxel in DE-MRI, and π_j denotes the proportion of the jth class. ψ is the PDF of single Gaussian component in GMM with mean u_j and variance σ_j. Once these parameters are determined, we obtain the clustering of DE-MRI, namely, the extraction of heart.

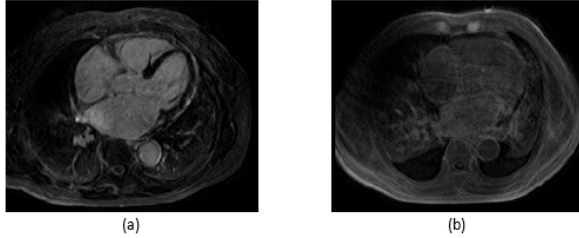(a)   (b)

Figure 2.   DE-MRI images of different patients. (a) DE-MRI with high contrast (b) DE-MRI with low contrast.

EM algorithm is a common method to solve this problem. It can automatically cluster the GMM by maximizing the posterior probability. However, as for the image shown in Fig. 2(b), heart region and surrounding lung, muscles are with similar intensity. Accurate extraction cannot be obtained when applying method based on intensity directly to such image. Noting that heart is the largest organ in the chest with intensity no less than surrounding tissues, we can locate the approximate center of the heart by:

$$(x_{cet}, y_{cet}) = \frac{\sum_{i=1}^{m}\sum_{j=1}^{n} I_{(i,j)}*(i,j)}{\sum_{i=1}^{m}\sum_{j=1}^{n} I_{(i,j)}} \quad (2)$$

where $I_{(i,j)}$ denotes the gray intensity of voxel located at (i, j). Experiment results show that the extraction results obtained by the approximate center are similar to those obtained by manually appoint. So we choose this method to reduce the manual intervention.

Then we use the following formula to generate the template image and fusion it with original image.

$$H(i,j) = \frac{\max(H) - \sqrt{(i-x_{cet})^2 + (j-y_{cet})^2}}{\max(H)} \quad (3)$$

$$I_{new} = w * I_{origin} + (1-w) * H \quad (4)$$

Template image H assigns higher gray intensity to the voxel closer to the center of heart, so the heart region can be obviously enhanced by fusing the original image and the template image. Thus a reasonable and complete extraction of heart is obtained by applying EM algorithm to the new image. Detailed result is shown at section III.

B. Segmentation of left atrial based on 3D level-set

The left atrial is consist of left atrial appendage, left atrioventricular port and left atrial sinus extended to the left and tight pulmonary vein portal. Due to the drastic contour change among slices and significant difference between patients, automated and accurate segmentation is hard to achieve. The level-set method is introduced to solve this problem. A prominent advantage of the level-set method is that it can simply represent contours of complex structures and can handle topological changes, such as splitting and fusing, which cannot be handled in many parametric active contour methods. In level-set method, the contour to be segmented is represented as a zero-level set of a higher dimensional function, called the level set function, and the change of the contour refers to the evolution of level set function. The general evolution equation is as follows:

$$\frac{\partial \phi}{\partial t} = F|\nabla \phi| \quad (5)$$

where ϕ is the time dependent level set function and F is the speed function that controls the motion of the contour. Abundant level-set method can be derived by defining different kinds of F. An efficient level-set method called distance regularized level set evolution (DRLSE) proposed by Li [7] is adopted in this paper. The evolution equation is defined as:

$$\frac{\partial \phi}{\partial t} = \mu \, div\left(d_\rho(|\nabla \phi|)\nabla \phi\right)$$
$$+ \lambda \delta_\varepsilon(\phi) div\left(g \frac{\nabla \phi}{|\nabla \phi|}\right) \quad (6)$$
$$+ \alpha g \delta_\varepsilon(\phi)$$

where d_p is a double-well potential function for distance regularization, δ_ε is the Dirac delta function and g is an edge indicator function. Based on the extraction of heart, the level set function can evolve in a smaller space, making the segmentation of LA achieved more rapid and accurate. Our results are shown in Fig. 3.
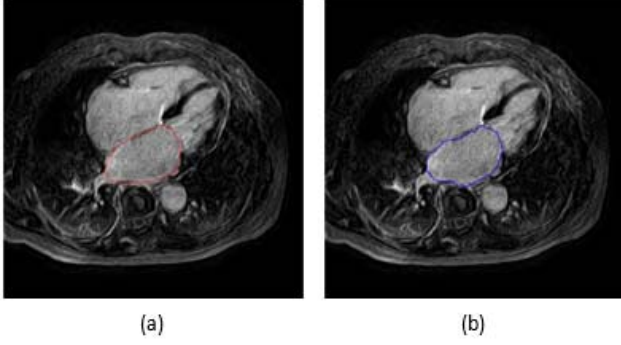
Figure 3. Segmentation of left atrial. The red line in (a) is the manual segmentation and the blue line in (b) is obtained by our method.

C. Quantification of fibrotic tissues based on k-means and graph-cut

Extraction of fibrotic tissues can be defined as assigning a label fp for every voxel p in the search space of the image. According to [8], the search space is defined as a region ±3 mm from the contour obtained from the segmentation of LA. By the prior knowledge, the fibrotic tissues have the highest gray intensity and a strip appearance regularly. In order to utilize the information of gray intensity and shape knowledge, we construct a graph model and use graph-cut to extract the fibrotic tissues.

Graph model maps the image into a weighted undirected graph G=<V, E>. In the graph, each node $\in$ V represents a voxel in image and each edge $\in$ E links a pair of adjacent voxel with a weight denotes the similarity. There are several terminal node represents the different classification. The principle of classify is to keep the voxels in each sub-graph maintaining the maximum similarity.

K-means is used to determine intensity of the terminal node and then the weight of link between a node and a terminal node is calculated by

$$T_c = (I_p - I_c)^2 \tag{7}$$

where I_p denotes the gray intensity of an arbitrary voxel p in image and I_c denotes gray intensity of the cth terminal node determined by k-means. The weight of edge linking adjacent voxels is calculated by

$$B_{pq} = e^{\frac{-(I_p - I_q)^2}{2\sigma}} \tag{8}$$

where σ denotes the variance of the whole search space. Then the minimum cut of the graph is obtained by the graph-cut algorithm. The class with highest gray intensity is extracted as the fibrotic tissues and furthermore the non-fibrotic tissues inside is removed by connectivity analysis.

In general, non-fibrotic tissue distribute massively in large area, which is different from the strip shape of fibrotic tissues. So we separate all the regions that are larger than a threshold, and calculation the ratio of major-axis to minor-axis. If the ratio is too small, this region is thought to be non-fibrotic tissues and should be removed. After the connectivity analysis

is finished, the proportion of fibrosis tissue in the left atrial wall could be calculated. Our results are shown in Fig. 4.
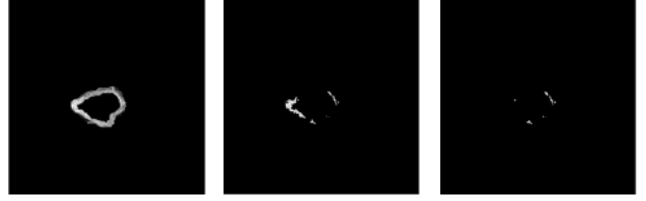

Figure 4. Results of graph-cut. The left image show the search space based on segmentation of LA. The middle image show the original extraction of fibrotic tissues and the right image show non-fibrotic tissues were removed by connectivity analysis.

III. MATERIALS AND RESULTS

A. Materials

1) Patients

In this study we selected 4 patients. The protocol was reviewed and approved by the Research Committees of Shanghai Chest Hospital, Shanghai Jiao Tong University (Shanghai, China) and a waiver was obtained for informed consent.

2) Data Acquisition

The Cardiac Magnetic Resonance (CMR) examination was performed on manufacturer's 5-channel 1.5 Tesla superconducting MR scanners (Achieva, Philips, The Netherlands) using a Sense-Cardiac coil with the patient in supine position, during expiratory apnea, and using electrocardiographic (ECG) gating. Intravenous infusion of gadolinium contrast (Magnevist; Bayer Healthcare 0.15 mmol/kg) was performed at an injection rate of 2 ml/s followed by a 20-30-mL saline flush. A vertical long-axis (VLA) modified look-locker inversion-recovery sequence (10 images within 12 heartbeats, slice thickness 6 mm, repetition time 8.0 ms, echo time 3.3 ms, flip angle 12 degrees, matrix 148 x 135, field of view 350 x 350 mm) was performed after contrast injection. Late enhanced MR imaging was performed fifteen minutes after the administration of gadolinium-DTPA intravenously (0.15 mmol/kg body weight) using inversion recovery 3D- Turbo field echo (TFE) with TE/TR 3.8/1.25 ms, matrix size 184×183, FOV 320×320, a flip angle of 15 degree, slice thickness 1.25mm) in maximum end enspiration position with breath hold.

B. Experimental results

We applied our method to the clinical DE-MRI image.3D level-set is adapted from the 2D demo shared by Li [9] and graph-cut is shared by Computer Vision Research Group at the University of Western Ontario [10].

1) Heart Extraction

According to the gray intensity level and anatomy, firstly we tried to classify the DE-MRI into three class (the background and chest, the muscle and lung, the heart). However, the extraction of heart is incomplete due to voxels with abnormal high gray intensity, which may be artifact or fibrotic tissues, as shown in Fig. 5(b). So we tune the number of class to 4 and extract the two classes with highest and

second highest gray intensity as the heart. Results are shown in Fig. 5.
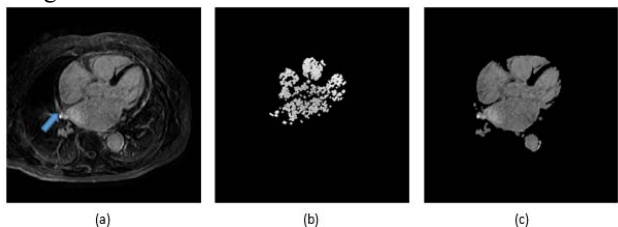

Figure 5. Result of heart extraction. (a) is the raw DE-MRI image with a blue arrow point to the voxel with abnormal high gray intensity. (b) is the incomplete extraction with class number 3 and (c) is the extraction with class number 4.

As for the image shown in the left column of Fig. 6, where heart region and surrounding lung, muscles have very similar gray intensity, we used our image enhancement method before classification. Contrast experiment results are shown in Fig. 6.
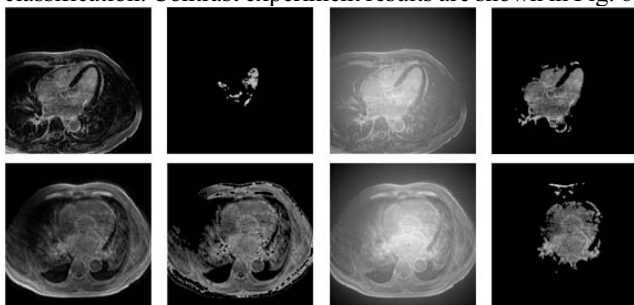

Figure 6. Extraction result of raw DE-MRI and enhanced DE-MRI. The left column are the raw DE-MRI and middle left column are the heart extracted from raw DE-MRI. The middle right column are enhance DE-MRI and the right column are the heart extracted from enhance DE-MRI.

Experiment results show that our enhancement method can effectively improve the extraction results of heart. Reasonable heart extraction is obtained in all 154 slices in 4 cases. One drawback is that the extraction results sometimes have small deletions in right atrial due to the approximate center we located is close to left atrial. But the purpose of the heart extraction is to serve the segmentation of the left atrial, so we deem that the results meet our expectations.

2) Segmentation of left atrial

According to the gradient parameter experiment, the optimal parameters in 3D level-set are set as follow: $\triangle t=10$, $\mu =0.02$, $\lambda =5$, $\alpha =-6$. Fig.7 show the segmentation results.

The image in the top row have good quality and distinct contour of left atrial. 3D level-set can trace the complex shape change and stop evolving at proper position, then achieve accurate segmentation of left atrial in its main body. Noting that if left atrial contain local high intensity region like the red arrow point to in the top row, a part of it should be included in initialization, otherwise level-set may stop at its boundary due to the inhomogeneity with other region. The shortcoming is that manual correction is still needed at the beginning and end slices of left atrial, where the shape change is drastic accompanied by change of topological like fusion and split. In

this case, automated and accurate segmentation are obtained in 20 slices with 31 slices in total.
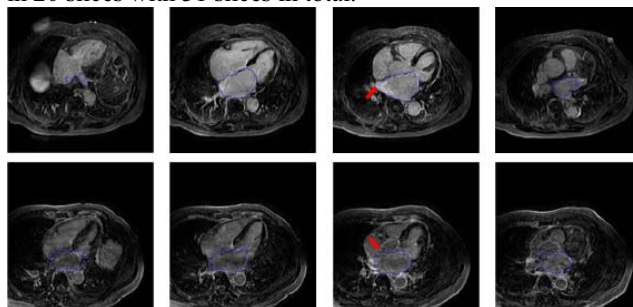

Figure 7. Results of segmentation of left atrial. Each row show 4 different silces of a patient. Blue lines show the contour of our segmentation result.

In the bottom row, the red arrow in the bottom row point to some blurry boundary causing a leakage in level-set and the whole image have a relatively poor quality compared to the top row. However we still get a continuous and accurate segmentation of left atrial because 3D level-set can utilize the information from the upper and lower slices. In this case, automated and accurate segmentation are obtained in 15 slices with 27 slices in total.

3) Quantification of fibrotic tissues

The thickness of left atrial wall is about 3 mm in anatomy and in the vicinity of left atrium wall, there are mainly the following four areas: blood pool, normal myocardium, pericardial fluid and fibrotic tissue. So the search space is defined as a region ±6 voxels from the contour obtained from the segmentation of LA and number of class is 4 in k-means. The threshold of non-fibrotic tissues is set to be 50 and threshold of ratio is 4. The results of extraction of fibrotic tissues is shown in Fig. 8.
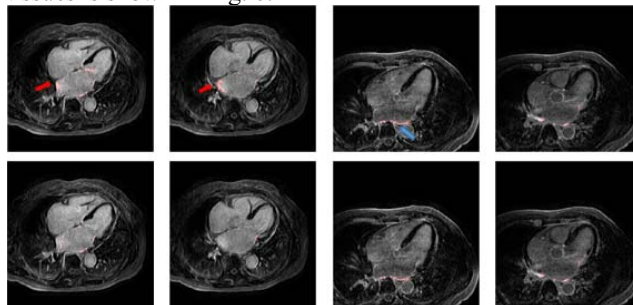

Figure 8. Result of extraction of fibroitc tissues. The top row show the results without connectivity analysis with red arrows pointing to non-fibrotic tissues and blue arrow pointing to fibrotic tissues. The bottom row show our final results.

Firstly, region with relatively high gray intensity is extracted as shown in the top row with pink color. Red arrows in the top row point to non-fibrotic tissues and blue arrow points to fibrotic tissues with large area. After connectivity analysis, the results are shown in the bottom row. We succeed in retaining the fibrotic tissues with large area and removing the non-fibrotic tissues. Then the results of proportion of fibrotic tissues in left atrial wall is shown in Table1. Evaluated by the clinician, our extraction of fibrotic tissues is reasonable

and the proportion calculated is consistent with clinical diagnosis.

TABLE I. PROPORTION OF FIBROTIC TISSUES IN LEFT ATRIAL

Number of patients	1	2	3	4
Proportion(%)	14.78	21.02	25.17	14.77

IV. CONCLUSION AND FUTURE WORK

In this paper, we propose a method for the segmentation of left atrial and quantification of fibrotic tissues with little manual intervention. The experimental results show that our method has satisfied performance on accurate segmentation of left atrial in its main body. Quantification of fibrotic tissues in left atrial can help designing individual treatment in ablation surgery. In general, our method can provide an auxiliary function to reduce the workload of clinician.

However, there are still some issues to deal with before put our method into application. First, as for segmentation of the beginning and end slices of left atrial where manual correction is needed, we hope to obtain prior knowledge about shape of left atrial by applying deep-learning in increased cases, so that level-set can trace the drastic shape change by combining with prior knowledge. In the quantification of fibrotic tissues, we hope to verify our method in more cases and further modify the method to improve the universality, then the 3D visualization technology could be used to provide more direct-viewing and comprehensive information about the fibrotic tissues for the clinician.

REFERENCES

[1] Yoko Miyasaka, Marion E. Barnes, Bernard J. Gersh, Stephen S. Cha,Kent R. Bailey, Walter P. Abhayaratna,James B. Seward, Teresa S.M. Tsang. Secular trends in incidence of atrial fibrillation in Olmsted County, Minnesota, 1980 to 2000, and implications on the projections for future prevalence.[J]. Circulation, 2006, 114(2):119-25.

[2] Badger T J, Adjeipoku Y A, Marrouche N F. MRI in cardiac electrophysiology: the emerging role of delayed-enhancement MRI in atrial fibrillation ablation.[J]. Future Cardiology, 2009, 5(1):63-70.

[3] Daniele Ravanelli, Elena Costanza dal Piaz, Maurizio Centonze, Giulia Casagranda, Massimiliano Marini,Maurizio Del Greco, Rashed Karim, Kawal Rhode, and Aldo Valentin. A novel skeleton based quantification and 3-D volumetric visualization of left atrium fibrosis using late gadolinium enhancement magnetic resonance imaging.[J]. IEEE Transactions on Medical Imaging, 2014, 33(2):566-576.

[4] Christian Wachinger, Karl Fritscher, Greg Sharp, and Polina Golland. Contour-Driven Atlas-Based Segmentation[J]. Medical Imaging IEEE Transactions on, 2015, 34(12):2492-2505.

[5] Qian Tao, Esra Gucuk Ipek, Rahil Shahzad, Floris F. Berendsen, Saman Nazarian, Rob J. van der Geest. Fully automatic segmentation of left atrium and pulmonary veins in late gadolinium-enhanced MRI: Towards objective atrial scar assessment.[J]. Journal of Magnetic Resonance Imaging, 2016, 40(2):315-315.

[6] Wang, R., Wang, J., Ding, J., & Zhang, S. Automatic Segmentation and Quantitative Analysis of Gray Matter on MR Images of Patients with Epilepsy Based on Unsupervised Learning Methods[M]// Trends and Applications in Knowledge Discovery and Data Mining. 2014:607-615.

[7] Chunming Li, Chenyang Xu, Changfeng Gui, Martin D. Fox. Distance regularized level set evolution and its application to image segmentation.[J]. IEEE Transactions on Image Processing A Publication of the IEEE Signal Processing Society, 2011, 19(12):3243-3254.

[8] Karim, R., Arujuna, A., Housden, R. J., & Gill, J. A Method to Standardize Quantification of Left Atrial Scar From Delayed-Enhancement MR Images[J]. Translational Engineering in Health & Medicine IEEE Journal of, 2014, 2(1):1-15.

[9] http://www.imagecomputing.org/~cmli/DRLSE/

[10] Andrew Delong, Anton Osokin, Hossam N. Isack, Yuri Boykov. Fast Approximate Energy Minimization with Label Costs[J]. International Journal of Computer Vision, 2012, 96(1):1-27.